5th International Conference on Materials and Reliability
Jeju, Korea, Nov. 27-29, 2019

High temperature low cycle fatigue behaviors of single crystal nickel- based superalloy with various orientations

J. Y. Song[1], J. H. Gu[1], M. H. Lee[1] and Y. W. Ma[1*]

[1]Materials Technology Department, Doosan Heavy Industries & Construction, Chang-won, Republic of Korea

[*]Corresponding author: youngwha.ma@doosan.com

1. Introduction

Single crystal (SC) nickel-based superalloys have been widely used for air craft gas turbine and industrial gas turbine engine, e.g. blade and vane because they have highly desirable material properties at high temperature, such as excellent resistance to creep, fatigue, and corrosion [1,2]. These outstanding high temperature mechanical properties of SC nickel-based superalloys derived from alloying element and unique microstructure. The microstructures consist of disordered gamma phase matrix (γ-FCC) and ordered gamma prime precipitates (γ'-Ni_3Al, $L1_2$ type) [3]. Usually, SC nickel-based superalloys possess large volume fracture of γ' precipitates approximately 50~60%.

During in service, industrial turbine engine components, blades and vanes, are exposed to high temperature atmosphere and subjected to thermal low cycle fatigue, creep-fatigue interaction and thermo-mechanical fatigue resulting from start-up and shut-down procedures [2,4]. This operating system induces temperature gradients, local thermal strains at turbine blades and vanes.

Therefore, it is very important to understanding of low cycle fatigue deformation/fracture mechanisms at high temperature.

Typically, gas turbine blades are subjected to multiaxial stress condition during actual service. It is certainly necessary to consider crystallographic dependence on low cycle fatigue property of SC nickel-based superalloys. Nevertheless, in the past several decades, many researchers have been carried out low cycle fatigue behavior along [001]. SC nickel-based superalloys as well as general SC alloy show anisotropic mechanical properties [5]. And these anisotropic mechanical properties were derived from different elastic modulus with different crystal orientation.

In the low cycle fatigue test, [001] direction specimens result in longest fatigue life because this direction has smallest elastic modulus. And with increasing elastic modulus, fatigue life gradually decreases [6].

In this work, high temperature low cycle fatigue behaviors of SC nickel-based superalloy with various crystal orientation ([001], [011], [111]) has been investigated. Also, we briefly discussed high temperature deformation mechanisms of SC nickel-based superalloy during high temperature low cycle fatigue.

2. Materials and experimental procedures

The investigated alloy is a SC nickel-based superalloy produced by investment casting. The nominal chemical composition of investigated alloy is shown in Table 1.

Table 1. Nominal composition of investigated alloy (wt.%)

Cr	Co	Al	Ti	W	Ta	Ni
12.7	9.0	3.2	4.2	3.9	3.9	Bal.

As-cast rods were subjected to solution heat treatment above γ' precipitate solvus temperature and subsequently two step heat treatment. After heat treatment, crystallographic orientation of SC nickel-based superalloy was measured by X-ray Laue back-reflection technique and it was selected within less than 6° from [001] orientation. [011] and [111] orientation samples were machined after tilted from [001] orientation to 45° and 54.7°.

Microstructure of all the directions were observed by optical microscopy (OM) and scanning electron microscopy (SEM), such as morphology, volume fraction and size distribution of γ' precipitates.

The low cycle fatigue specimens with a diameter of 5 mm and a gauge length of 14 mm were machined parallel to the [001], [011] and [111] direction. Before fatigue test, all specimens were subjected to mechanical polishing in order to eliminate the effects of surface defects. The detailed geometry of LCF specimen is shown in Fig. 1. (unit: mm)

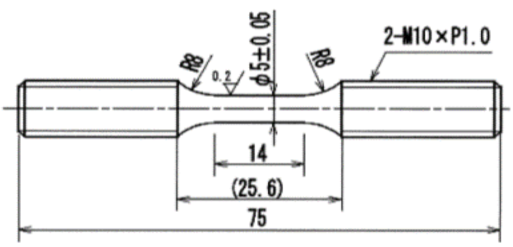

Fig. 1 Geometry of the low cycle fatigue specimen.

Low cycle fatigue tests conducted at 950'C with a servo hydraulic testing machine, MTS810, under total axial strain control. Total strain was controlled by an extensometer (gage length: 12 mm) mounted on the ledges of the specimens. A fully reversed triangular waveform was conducted to achieve various strain amplitudes at a constant strain rate 1 x 10^{-3} s^{-1} and strain ratio (R_ε) = -1 was used. After fatigue test, fracture surfaces were observed using SEM with all sample directions.

3. Results and discussion

The low cycle fatigue results with various sample direction were shown in Fig. 2. All samples show that fatigue resistance significantly decreased with increasing strain amplitude levels. And it is significantly related to orientation. The relationship of total strain amplitude, plastic strain amplitude, elastic strain amplitude was expressed by Eq. (1) combined with the Basquin and Coffin-Manson relationship as follow:

$$\Delta\varepsilon_t/2 = \Delta\varepsilon_e/2 + \Delta\varepsilon_p/2 = \sigma_f'/E(2N_f)^b + \varepsilon_f'(2N_f)^c$$

Where σ_f' and b are fatigue strength coefficient, and exponent. ε_f' and c are fatigue ductility coefficient and exponent, and E is Young's modulus achieved from stable cycle (approximately half cycle). The fatigue parameters were shown in Table 2.

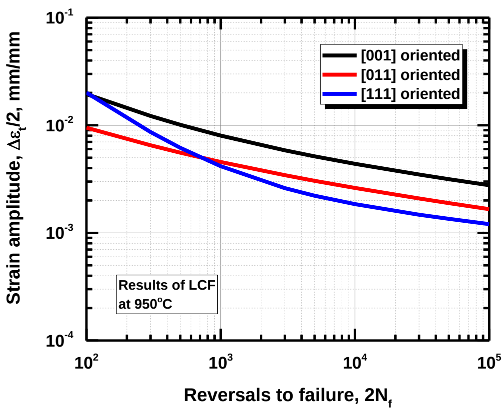

Fig. 2 The Basquin and C-M relationship between total strain amplitude and reversals to failure.

Table 2. Low cycle fatigue parameters of alloys with various orientation.

Direction	σ_f'/E	b	ε_f'	c
[001]	0.0176	-0.1635	0.2557	-0.6795
[011]	0.0101	-0.1615	0.0660	-0.5740
[111]	0.0060	-0.1408	1.3536	-0.9509

Cyclic stress response curves with various orientation is shown in Fig. 3. Cyclic stresses are increased as follows, [111] > [011] > [001]. It is found that fatigue life is significantly related to orientation and strain amplitude. Cyclic stress responses of alloy with various orientations show cyclic softening behavior without cyclic hardening until fracture. This cyclic stress behavior is significantly related to elastic modulus and slip system. Fig. 4 shows cyclic elastic modulus of alloy with various specimen direction [001], [011], [111]. Elastic modulus rapidly increased from [001] to [111]. [001] specimen shows lowest cyclic elastic modulus. And [111] specimen was required high stress to deformation than that of [001] and [011] specimens.

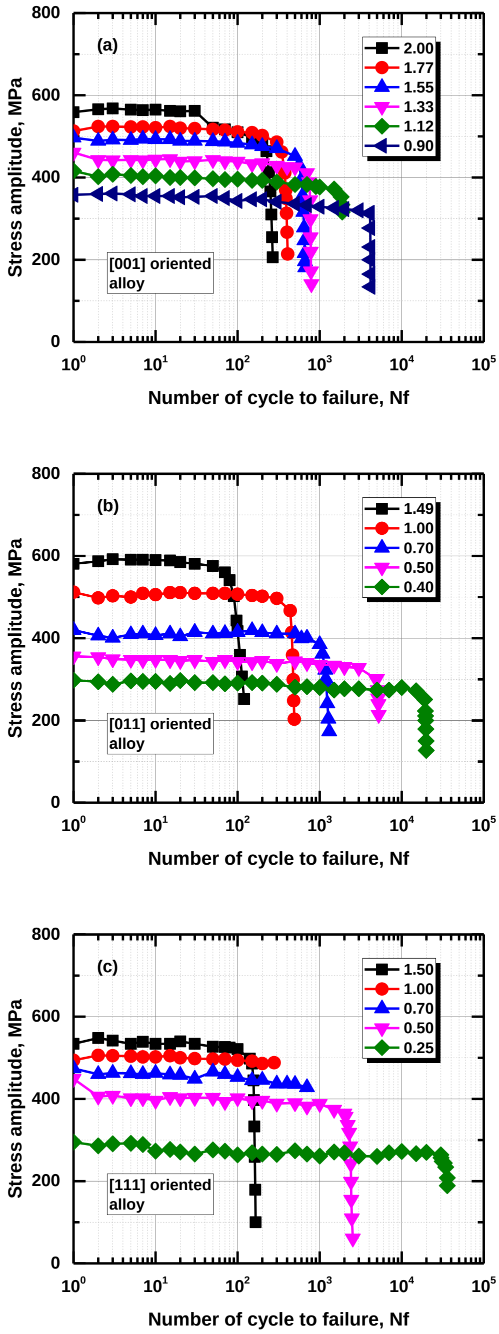

Fig. 3 Cyclic response curve of the alloy with orientations of (a) [001], (b) [011] and (c) [111].

In order to determine the different elastic modulus, Schmid factor and active slip system were calculated using [001], [011], [111] specimens, and results were shown in Table 3. [001], [011] specimens have same Schmid factor while [001] specimen has a lot of active slip system than that of [011] specimen. [111] specimen has lowest Schmid factor and active slip system among three kind of direction. Therefore, [111] specimen shows lowest fatigue life and highest elastic modulus.

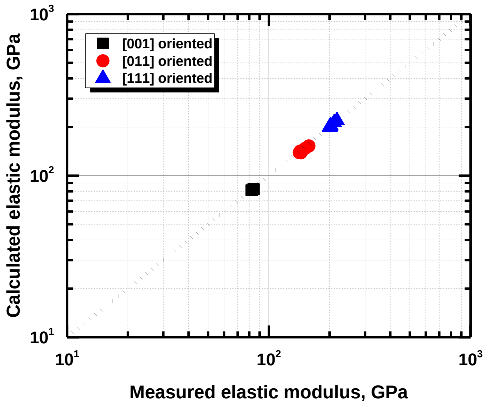

Fig. 4 Comparison between calculated and measured cyclic elastic modulus with various specimen direction.

Table 3. Calculated Schmid factor (S.F) and active slip system with various specimen direction.

	Slip plane			Slip direction			S.F
[001]	1	1	1	-1	0	1	0.408
	1	1	1	0	1	-1	-0.408
	1	1	-1	1	0	1	-0.408
	1	1	-1	0	1	1	-0.408
	1	-1	1	1	0	-1	-0.408
	1	-1	1	0	1	1	0.408
	-1	1	1	1	0	1	0.408
	-1	1	1	0	1	-1	-0.408
[011]	1	1	1	1	-1	0	-0.408
	1	1	1	-1	0	1	0.408
	-1	1	1	1	1	0	0.408
	-1	1	1	1	0	1	0.408
[111]	1	1	-1	1	0	1	0.272
	1	1	-1	0	1	1	0.272
	1	-1	1	1	1	0	0.272
	1	-1	1	0	1	1	0.272
	-1	1	1	1	1	0	0.272
	-1	1	1	1	0	1	0.272

Macro-fracture surfaces after high temperature low cycle fatigue test are shown in Fig. 5(a), (b), (c). Macro-fracture surfaces are similar regardless crystallographic orientations. Relatively high strain specimens regardless of orientation show oblique fracture surfaces. However, oblique fracture surfaces were disappeared with decreasing strain. Most specimens regardless of crystal orientation have flat macro-fracture surfaces. These flat macro-fracture surfaces are significantly related to dislocation movement. Also, it can be explained interaction between dislocation and γ' precipitates. Consequently, SC nickel-based superalloys show similar deformation mechanisms regardless of crystal orientation. At this high temperature, dislocation continues to move bypass the γ' precipitates and begins to climb with freedom [7, 8].

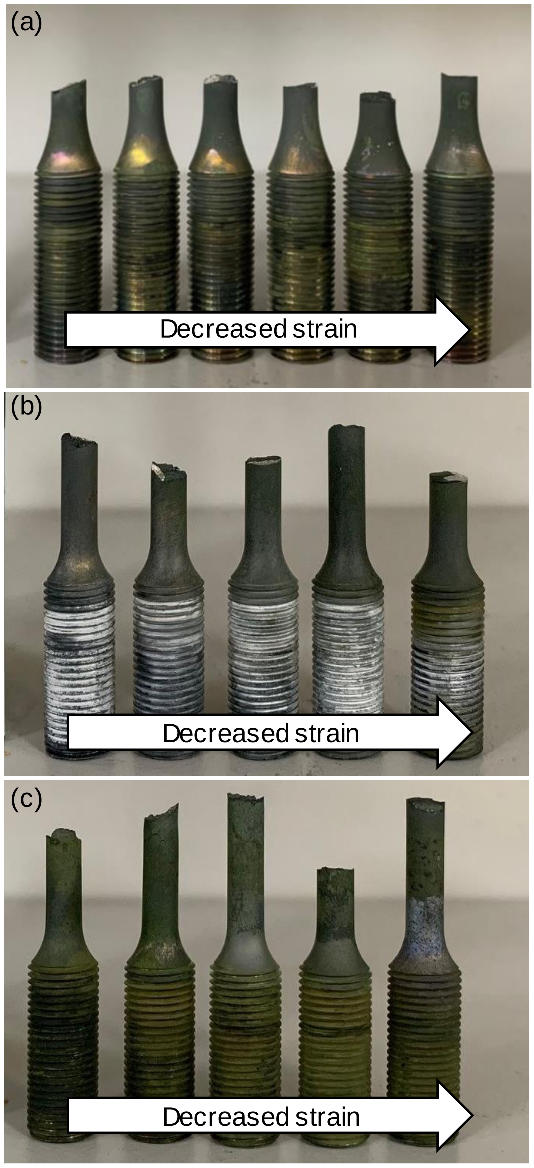

Fig. 5 Schematic of fractured specimens with various crystal orientation, (a) [001] (b) [011], (c) [111]

4. Conclusions

The effect of orientation on the low cycle fatigue at 950'C of SC nickel-based superalloy was studied. The conclusions are as follows:

(1) The [001] oriented alloy shows longest fatigue life than those of [011], [111] oriented alloy. The [111] oriented alloy exhibits shortest fatigue life.

(2) The cyclic stress responses are significantly dependent upon strain amplitude levels and orientation. All conditions show that cyclic softening behavior to failure cycle without cyclic hardening behavior. It is due to dislocation configuration at this temperature.

(3) Elastic modulus is significantly dependent on crystallographic orientation. [111] oriented alloy shows highest elastic modulus than those of [001], [011] oriented alloys.

Acknowledgment

This work was supported by Korea Institute of Energy Technology Evaluation and Planning (KETEP) grant funded by Korea government Ministry of Knowledge Economy. (No.2013101010170C)

References

[1] R.C. Reed, The superalloys: Fundamentals and applications, Cambridge University Press, 2008
[2] X.G. Wang et al. Dependence of stacking faults in gamma matrix on low cycle fatigue behavior of a Ni-based single crystal superalloy at elevated temperature, Scr. Mater. 152, (2018), 94-97
[3] F. Pyczak et al. The influence of different alloying elements on the development of the gamma/gamma prime microstructure of nickel-base superalloys during high temperature annealing and deformation, Acta Mater, 53 (2005), 3879-3891
[4] H.U. Hong et al. A comparative study on thermomechanical and low cycle fatigue failures of a single crystal nickel-based superalloy, Int. J. Fatigue, 33 (2011) 1592-1599
[5] D. Shi et al. Effects of crystallographic orientations and dwell types on low cycle fatigue and life modelling of a SC superalloy, Int. J. Fatigue, 49 (2013), 31-39
[6] L. Liu et al, Effects of crystal orientations on the cyclic deformation behavior in the low cycle fatigue of a single crystal nickel base superalloy, Mater. Des. 131 (2017) 441-449
[7] P. Li et al. Comparison of low cycle fatigue behaviors between two nickel-based single crystal superalloys, Int. J. Fatigue 63, (2014) 137-144
[8] Z. He et al. Temperature effect on the low cycle fatigue behavior of a directionally solidified nickel-based superalloy, Mater. Sci. Eng. A 676, (2016), 246-252